Journal of Magnetism and Magnetic Materials 475 (2019) 146–151

Contents lists available at ScienceDirect

Journal of Magnetism and Magnetic Materials

journal homepage: www.elsevier.com/locate/jmmm

Research articles

# Study of Brownian motion of magnetic nanoparticles in viscous media by Mössbauer spectroscopy

Raul Gabbasov[a,*], Anton Yurenya[a], Alexey Nikitin[b], Valery Cherepanov[a], Michael Polikarpov[a], Michael Chuev[a,c], Alexander Majouga[b], Vladislav Panchenko[a]

[a] National Research Center "Kurchatov Institute", Moscow, Russia
[b] National University of Science and Technology "MISiS", Moscow, Russia
[c] Valiev Institute of Physics and Technology, Russian Academy of Sciences, Moscow, Russia

ARTICLE INFO

*Keywords:*
Mössbauer spectroscopy
Superparamagnetic nanoparticles
Brownian motion
Instant velocities

ABSTRACT

The Mössbauer spectroscopy method was used to study the Brownian motion of magnetic nanoparticles in viscous media of glycerol solution, simulating cell cytoplasm. We used samples of two types of ferrofluids based on the magnetite nanoparticles with average hydrodynamic sizes 140 and 40 nm. The nanoparticles were enriched by $^{57}$Fe isotope to compensate the decrease of the Mössbauer effect probability in the liquid media. In order to maximize the viscosity coefficient we dissolved both samples in glycerol to receive more than 90% glycerol solution. We carried out two experimental series at different temperatures on ferrofluids dissolved in glycerol and ferrofluids dried to the powder-state to exclude the influence of the temperature dependent Neel relaxation. The analysis of the spectra allowed us to reveal the Brownian movement of the particles and to evaluate intrinsic dynamical parameters of the model viscous medium.

## 1. Introduction

Ferrofluids composed of magnetic nanoparticles became increasingly important for technical and medical applications and are used today in many industrial, scientific and medical applications including drug delivery, gene therapy, magnetic hyperthermia, contrasting of the magnetic resonance images (MRI) [1–5]. The high-frequency magnetic properties of nanoparticles and their relaxation rate are determined by two different relaxation mechanisms. One of them is intrinsic Neel relaxation process leading to a coherent rotation of the nanoparticle's spin as a single magnetization vector between directions of easy magnetic anisotropy axes. Another mechanism involves the Brownian motion of nanoparticles which may cancel the net magnetic moment of the nanoparticles by spatial rotation in the fluid. The possibility of the remote manipulation of magnetic nanoparticles and their functional behavior in the body are determined both by the properties of the ferrofluid which can be controlled by synthesis procedure and by the characteristics of their Brownian motion in a target region. The study of a short-range Brownian motion opens up a completely new direction in biological research [6]. The transport processes at the cellular level exceeds by a few orders of magnitude in its value expected from the theory, which is explained by the phenomenon of anomalous diffusion [7]. A conclusive test of the nature of the translational motion in cells is missing owing to the lack of techniques capable of probing intracellular fluids with the required temporal and spatial resolution. In 1905 Albert Einstein derived a formula expressing the average displacement x of Brownian particle in fluid as $< x^2(t) > = 2Dt$, where D - diffusion constant of the fluid [8]. Using this equation, it is possible to derive the average velocity as

$$<v(t)> = \sqrt{2D/t} \quad (1)$$

When the time $t$ approaches to zero the average velocity can be considered as instantaneous and according to the eq.1 it becomes infinite. However, this approach is valid only for long time period when the particle undergoes a large number of collisions. For the small times, in the so called ballistic regime when collisions are very rare, the motion of the Brownian particle is mainly determined by inertia. It should be noted that this time range has a great practical importance for such applications as magnetic hyperthermia and magnetic resonance imaging, which are based on high-frequency magnetic properties of nanoparticles.

There are only a few works in which the instantaneous Brownian velocities were studied because of the high demands of the spatial and temporal resolution. It was reported about a direct measurement of the

* Corresponding author.
*E-mail address:* gabbasov_rr@nrcki.ru (R. Gabbasov).

https://doi.org/10.1016/j.jmmm.2018.11.044
Received 24 June 2018; Received in revised form 6 November 2018; Accepted 6 November 2018
Available online 13 November 2018
0304-8853/ 

Brownian velocities of nanoparticles by optical tweezer method in air [9] and then in water and acetone [10]. This method requires transparent environment with low impurities concentration, which cannot be applicable to the complicated biological systems such as cell cultures. Another method, which can be highly sensitive to the instantaneous Brownian velocities, is Mössbauer spectroscopy method. The direct observation of the Mössbauer effect in the ferrofluids with magnetic nanoparticles involved in the Brownian motion is a challenging task because the high Brownian velocities may easily nullify the recoilless absorption probability. The most obvious way to handle this problem is to significantly increase the size of nanoparticles which leads to the decrease of the Brownian velocities magnitude. Since the discovery of the Mössbauer effect in 1958 in a number of works Mössbauer spectra of microparticles in various liquids such as distillated water, acetone or glycerol solutions, etc. were obtained [11–14]. Another approach consists of increasing the viscosity of the liquid. The Brownian velocities are reversely proportional to the viscosity coefficient, which can be controlled by temperature or a solution composition.

In this work we demonstrated the ability of Mössbauer spectroscopy to study the Brownian motion of magnetic nanoparticles in viscous media simulating cell cytoplasm. The most suitable media for this role is glycerol which is water-soluble and has a high viscosity, which exponentially increases with decreasing temperature. However, the freezing point of glycerol and its viscosity strongly depends on the rate of cooling [15]. In order to exclude the possibility of crystallization of glycerol at low temperatures (in the order of 240 K) and to obtain a liquid of high viscosity, the samples of nanoparticles were rapidly cooled (with the rate more than 4 K /min) to the required temperature point. We used samples of the ferrofluid based on the magnetite nanoparticles with average hydrodynamic sizes 140 (N1) and 40 nm (N2). In order to maximize the viscosity coefficient we dissolved both samples in glycerol to receive more than 90% glycerol solution. The nanoparticles were enriched by $^{57}$Fe isotope to compensate decreasing of the probability of the Mössbauer effect in the liquid media. The influence of the Brownian motion on the Mössbauer spectra in the first approximation can be considered as uniform broadening of all spectral lines [11,14]. In the above-mentioned works the Mössbauer spectra of liquid-state samples containing nano- or microparticles were usually collected at various temperature points to show the temperature dependence of this line broadening. It should be noted, this spectral line broadening is a result of superposition of two different processes of the Brownian motion and the Neel relaxation. The method of separation of these processes firstly was proposed in the work [16]. It is based on a joint analysis of the Mössbauer spectra of two samples, in one of which both processes take place, and in the other only the process of Neel relaxation. For these reasons we carried out an additional experimental series with the dried ferrofluid of the same nanoparticles, in which the Brownian motion was absent in order to exclude the influence of the temperature dependent Neel relaxation.

## 2. Experimental details

### 2.1. N1 synthesis

The mixture of $^{57}$Fe oleate complex (4 mmol, 96% $^{57}$Fe enrichment), NaOL (1.3 mmol) and OA (1.3 mmol) were dissolved in 1-octadecene (33 ml), heated to 140 °C under argon flow and vigorous stirring (4000 rpm) and then the system was heated at a rate of 4 °C/min to the reflux temperature and refluxed under argon atmosphere for 30 min. The resulting solution was cooled down to room temperature and 2-propanol was added to precipitate MNs. Finally, MNs were separated by centrifugation and redispersed in hexane. To produce stable water dispersion MNs were covered with Pluronic F-127: Pluronic F-127 (6 μmol) was dissolved in water (4 ml) and MNs in hexane with iron concentration [$Fe_3O_4$] = 4.0 mg/ml (1 ml) were added to this solution. Resulting mixture was sonicated for 5 min and stirred during 24 h. Then

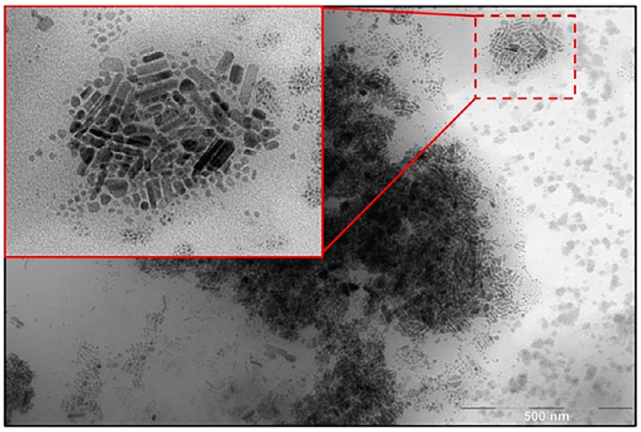


**Fig. 1.** TEM and HRTEM images of $^{57}Fe_3O_4$ oleate nanoparticles (N1 type).

MNs covered with Pluronic F-127 were collected from reaction mixture by ultracentrifugation (14000 rpm) and redispersed in water. This procedure was repeated three times [18].

### 2.2. N2 synthesis

Was performed according to the coperspiration method described by Massart [19]. Iron salts were mixed in a ratio of 20 ml of 1 M $^{57}FeCl_3$ solution (96% $^{57}$Fe enrichment) to 5 ml of 2 M $FeCl_2$ solution. The resulting solution was poured into 250 ml of 0.7 M $NH_4OH$ and stirred vigorously for 30 min. The obtained nanoparticles were precipitated in the presence of a magnetic field and stabilized with citric acid.

### 2.3. Nanoparticles characterization

The structure and morphology of the synthesized nanoparticles were studied by transmission electron microscopy (TEM) and high-resolution TEM (HRTEM) transmission electron microscopy (JEOL JEM-2100). The TEM and HRTEM images are shown on Fig. 1 and Fig. 2. The hydrodynamic size of the conjugated N1 nanoparticles was measured by dynamic light scattering using a Malvern Zetasizer Nano-ZS (Fig. 3). To do this, 1 ml of an aqueous solution of the nanoparticles with a concentration of iron [Fe] = 1 mg·ml$^{-1}$ was placed in a cuvette with size 10 × 10 mm). It can be seen that the nanoparticles have a good monodispersity as evidenced by the low polydispersity index value (PDI = 0.16).

### 2.4. Mössbauer samples preparation

The N1 and N2 nanoparticles have more than 96% and 63% $^{57}$Fe enrichment correspondingly. Each of these types of nanoparticles was used to prepare a dried sample (in rotary evaporator till powder state) and a liquid sample. The liquid samples were made by dissolving colloids of nanoparticles in 99% glycerol to receive 90% glycerol solution.

### 2.5. Mössbauer spectra

Of all samples were measured in the temperature range of 240–296 K with moving absorber geometry. The radioactive source $^{57}$Co (Rh) was used as the γ – radiation emitter. Isomer shifts were determined relative to the absorption line of α-Fe. The analysis of all Mössbauer spectra was carried out in the frame of many-state model formalism [20,21] with assumption of two different crystal sublattices whose corresponds to the two sextets in the spectra.

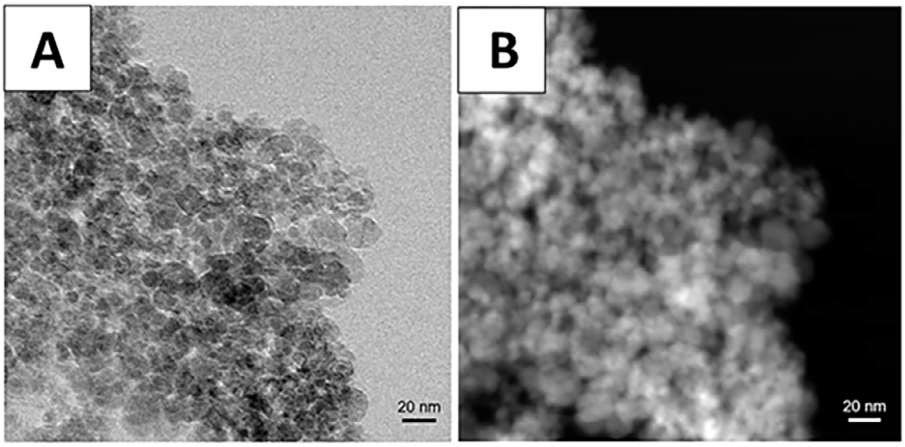


**Fig. 2.** TEM images of $^{57}Fe_3O_4$ citrate coated nanoparticles (N2 type). Dark field (A) and white field (B).

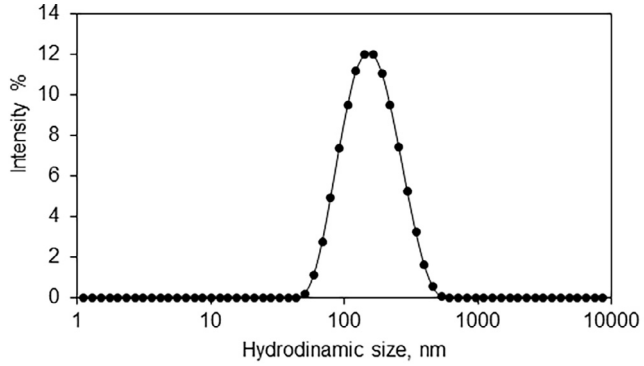


**Fig. 3.** Hydrodynamic size of magnetic $^{57}Fe$ oxide nanoparticles (N1 type) after conjugation with Pluronic F-127 copolymer.

## 3. Results

The morphology of the obtained N1 magnetic nanoparticles was carried out using transmission electron microscopy. From the obtained micrographs, it can be seen that the obtained nanoparticles have a rod-like shape (Fig. 1). The morphology of the magnetic nanoparticles coated with citrate ions (N2 type) was established using transmission electron microscopy. The sample was analyzed in light and dark fields (Fig. 2). From the obtained micrographs, one can see that the nanoparticles have high monodispersity.

The Mössbauer spectra of the dry samples of N1 type have well-resolved hyperfine structure at all temperatures (Fig. 4). There is a constant growth of the spectral linewidth with temperature caused by the Neel relaxation. The room "dry" spectrum contains a strong line splitting near V = −7 mm/s caused by big difference of hyperfine fields of magnetic sublattices, which points to the big (25 nm and more) crystalline size of the N1 nanoparticles [24,25]. At 240 K the difference between the "dry" and "liquid" spectra of N1 nanoparticles almost disappears because of the tremendous viscosity coefficient. However, the sample is still in liquid state at this temperature. The temperature evolution of the "liquid" sample demonstrates more intensive broadening than the "dry" one caused by the Brownian motion which leads to the difference between the linewidths (~0.5 mm/s) of the "dry" and "liquid" samples at room temperature. This difference is cause by the Brownian motion which is effectively broadening the Mössbauer spectra of the liquid sample. However, because of the relatively large hydrodynamic size (140 nm) the influence of the Brownian motion is not considerable comparing to the N2 sample with much smaller hydrodynamic size (≈40 nm). The "dry" sample of N2 type nanoparticles (Fig. 5) has the similar temperature behavior as the dry" one prepared from N1 type particles. As the temperature rises, the magnetic hyperfine structure of all Mössbauer spectra starts broadening due to thermal activation of the excited energy levels of the magnetization vectors of magnetic nanoparticles, which leads to the appearance of asymmetric lines with sharp external fronts and internal fronts that are strongly smeared toward the center of the spectrum [23].

## 4. Discussion

The spectral linewidth usually grows with temperature because of the superparamagnetic relaxation of nanoparticles magnetic moments. This takes place both in the "dry" and "liquid" samples. However, there is an additional line broadening in "liquid" samples caused by the Brownian motion $\Delta\Gamma_B$ which can be expressed by [11,14]

$$\Delta\Gamma = \frac{E_0^2 k_B}{3\hbar\pi c^2}\frac{T}{R\eta} \quad (2)$$

where T – temperature, η – viscosity coefficient, R – nanoparticles hydrodynamic size. The increase in the spectral line broadening upon rising temperature given by (2) relates to the temperature dependence of viscosity coefficient η,

$$\eta(T) = \eta_0 e^{W/k_B T} \quad (3)$$

where $\eta_0$ is a constant, W the activation energy of the viscous media, and $k_B$ the Boltzmann constant. The "dry" and "liquid" spectra both of the spectra (Figs. 4 and 5) at the same temperature were fitted simultaneously with the same set of spectral parameters [22], except the spectral linewidth. In other words, the widths of the "liquid" spectra and the "dry" spectra were calculated independently. Consequently, the additional line broadening related to the Brownian motion can be expressed by

$$\Delta\Gamma_B(T) = \Gamma_{Br+Neel}(T) - \Gamma_{Neel}(T) = \Gamma_{liq}(T) - \Gamma_{dry}(T) \quad (4)$$

The "liquid" samples demonstrate a considerable broadening, which can be explained by fast velocities of nanoparticles involved in the Brownian motion. As the result at room temperature, the hyperfine structure in the spectra almost disappears because of the significant (more than 1.5 mm/s) spectral linewidth broadening. Another factor weakening the Mössbauer spectra intensity, which can be observed on the Fig. 5, is decrease of recoilless absorption probability because of the finite size of isolated nanoparticle flowing in the fluid. During the resonance absorption of the gamma quanta the recoil momentum from the photon is transmitted to the whole nanoparticle, which mass is much bigger than the mass of the single atom. Furthermore, in the usual conditions, when the studying sample has the powder state of frozen, the position of nanoparticle is fixed by neighbor nanoparticles. As the result the recoil velocity becomes negligible and cannot effect on the

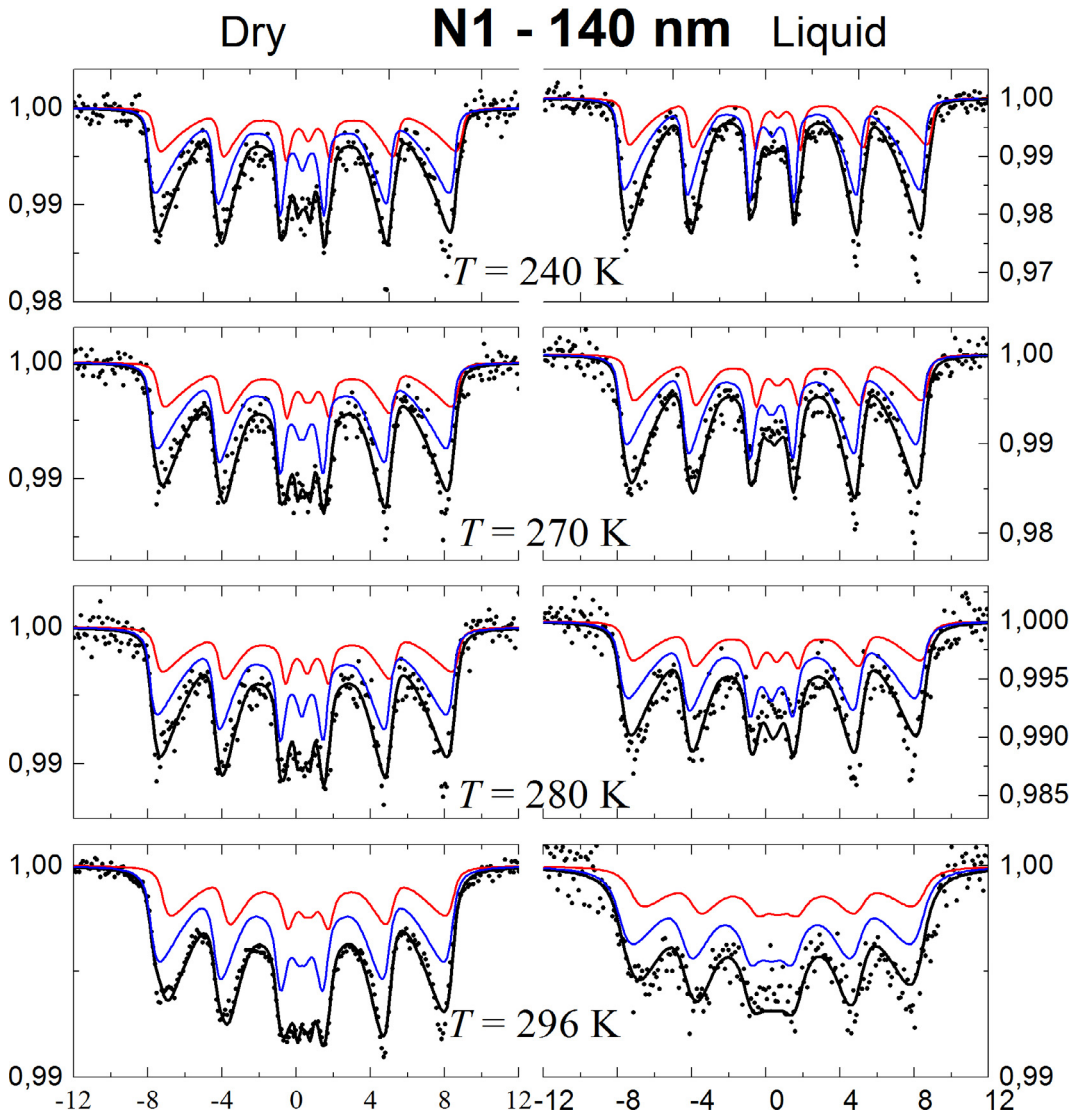


**Fig. 4.** $^{57}$Fe Mössbauer spectra of "dry" (left) and "liquid" (right) samples prepared from N1 nanoparticles. Red and blue lines correspond to two crystal sublattices. Dark lines describe resulting spectra. (For interpretation of the references to colour in this figure legend, the reader is referred to the web version of this article.)

probability of the Mössbauer absorption. On the opposite, the N2 nanoparticles floated in the glycerol were isolated by stabilization procedure during the synthesis and then sonicated. As the result the recoil momentum is transmitted to the nanoparticle with outer size about 40 nm and the recoil velocity has the nonzero value and effectively decreases the probability of the Mössbauer effect.

It should be noted that the spectral line broadening according to formula (2) is inversely proportional to the size of the nanoparticles. Therefore, in the case of a polydisperse nanoparticle sample, the Mössbauer spectrum will be a superposition of a large number of subspectra, with various line shapes due to different relaxation rates of nanoparticle magnetization vectors. However, the smaller nanoparticles will suffer from the effect of decreased probability described above, i.e. the contribution to the spectrum from the small nanoparticles will be less noticeable than the contribution from the large nanoparticles. As the result, it makes the discussed method weakly sensitive to the sample polydispersity.

Using the formula (4) it is possible to obtain temperature dependence of the Brownian line broadening for the N1 and N2 nanoparticles (Fig. 6). At 240 K the difference between the "dry" and "liquid" spectra for both types of nanoparticles almost disappears because of the tremendous viscosity coefficient. It should be noted that characteristics of the glycerol solution for the N1 and N2 were identical, which means that any difference between their Brownian line broadening can only be explained by the different hydrodynamic sizes. The Brownian line broadening $\Delta\Gamma_B$ for the N1 nanoparticles grows practically exponential with temperature, which can be explained by the temperature dependence of the viscosity coefficient in (3). On the other hand, the $\Delta\Gamma_B$ parameter for the N2 nanoparticles demonstrates linear growth rate. The Brownian line broadening $\Delta\Gamma_B$ can be used to estimate the diffusion coefficient $D_{NP}$ of the nanoparticles in the glycerol solution according to the formula [17]:

$$D_{NP} = \frac{\hbar c}{2E_0^2}\Delta E_B \tag{5}$$

where $\Delta E_B$ is the energy equivalent of the Brownian line broadening $\Delta\Gamma_B$, determined by equation

$$\Delta E_B = \frac{E_0}{c}\Delta\Gamma_B \tag{6}$$

The final expression for diffusion coefficient takes the form

$$D_{NP} = \frac{\hbar c}{2E_0}\Delta\Gamma_B \tag{7}$$

Using the experimental data it is possible to calculate the diffusion

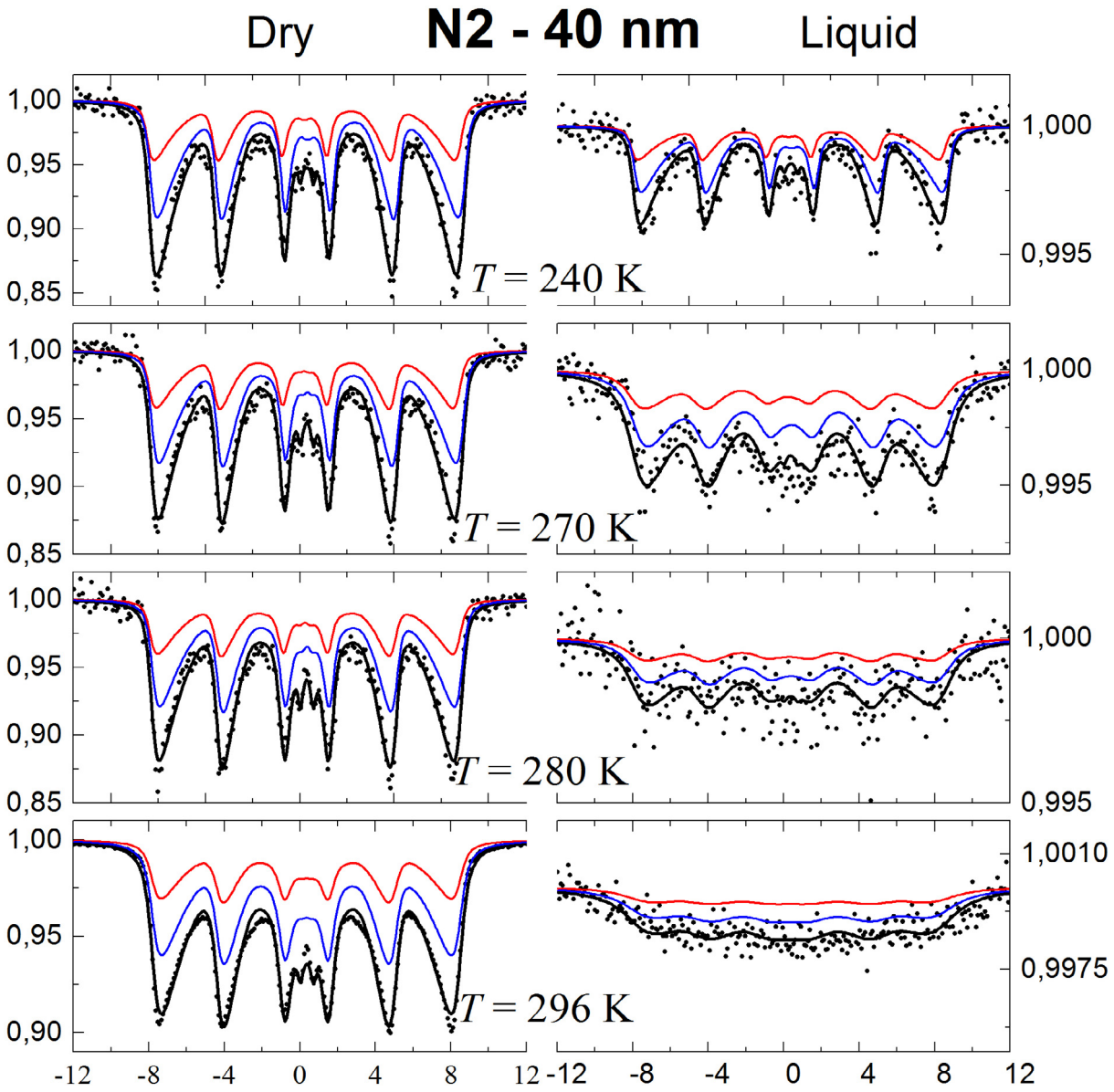


**Fig. 5.** $^{57}$Fe Mössbauer spectra of "dry" (left) and "liquid" (right) samples prepared from N2 nanoparticles. Red and blue lines correspond to two crystal sublattices. Dark lines describe resulting spectra. Mössbauer experimental data at temperatures of 240 K, 270 K, and 296 K were taken from [16]. (For interpretation of the references to colour in this figure legend, the reader is referred to the web version of this article.)

coefficient of N2 nanoparticles in glycerol solution, which is roughly equals $1.4 * 10^{-14}$ m$^2$/sec. This value is three orders lesser than the diffusion coefficient of the 100% glycerol $1.4 * 10^{-11}$ m$^2$/sec at temperature 25 °C received in work [26].

To track more accurately the temperature dependence of the Brownian line broadening $\Delta\Gamma_B$ the Eq. (2) should be rewritten to account for the temperature dependence of viscosity coefficient

$$\frac{\Delta\Gamma}{k_B T} = \frac{E_0^2}{3\hbar\pi c^2}\frac{e^{-W/k_B T}}{R\eta} \tag{9}$$

After taking the logarithm of the both sides it gives us the formula:

$$\ln\left(\frac{\Delta\Gamma}{k_B T}\right) = \frac{A}{T} + B \tag{10}$$

where $A = -\frac{W}{k_B}$ and $B = \ln(\frac{E_0^2}{3\hbar\pi c^2}\frac{1}{R\eta_0})$are constants determined by the media.

The Fig. 7 demonstrates reverse temperature dependence of the new parameter (7). Because of the very high relative errors ($\Delta\Gamma_B \sim 0$), the parameters at 240 K were not used. These dependences for both nanoparticle types are linear, which validates in the first approximation the Eq. (2) for the Brownian spectral line broadening in the fluids with high viscosity.

## 5. Conclusion

The developed method for analyzing the Mössbauer spectra of magnetic nanoparticles in viscous media based on the relaxation dynamical model of the Néel ensemble of ferrimagnetic single-domain particles describes the experimental spectra with good quality. the spectral line broadening and the probability of the Mössbauer effect in liquid media are significantly depend on both the hydrodynamic size of nanoparticles suspended in the liquid and the dynamic viscosity coefficient of the liquid in accordance with theoretical predictions. The simultaneous analysis of the "dry" and "liquid" samples allowed one to separate the contributions of the Brownian motion and the Neel relaxation to the spectral line broadening. The intrinsic parameters of the

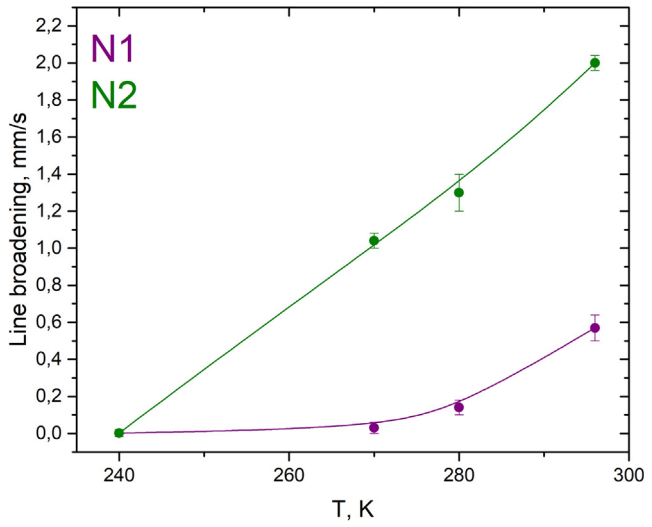


**Fig. 6.** Temperature dependence of Brownian line broadening for N1(blue) and N2 (red) nanoparticles. (For interpretation of the references to colour in this figure legend, the reader is referred to the web version of this article.)

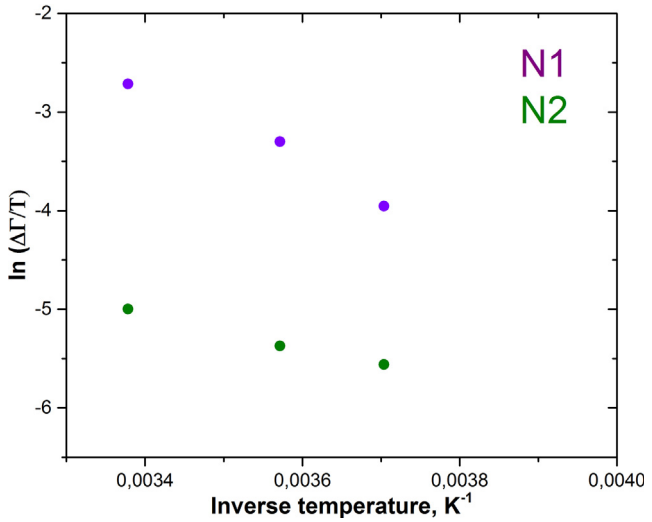


**Fig. 7.** Modified dependence of the Brownian line broadening for N1 (purple) and N2 (green) nanoparticles. (For interpretation of the references to colour in this figure legend, the reader is referred to the web version of this article.)

viscous medium can be evaluated from the analysis of the corresponding Mössbauer spectra.

## Acknowledgment

The work was partly supported by the Russian Foundation for Basic Research under the Grant 17-00-00438.

## References

[1] O. Veiseh, J.W. Gunn, M. Zhang, Design and fabrication of magnetic nanoparticles for targeted drug delivery and imaging, Adv. Drug Deliv. Rev. 62 (3) (2010) 284–304.
[2] H. Khurshid, S.H. Kim, et al., Development of heparin-coated magnetic nanoparticles for targeted drug delivery applications, J. Appl. Phys. 105 (7) (2009) 308–315.
[3] Q.A. Pankhurst, et al., Progress in applications of magnetic nanoparticles in biomedicine, J. Phys. D: Appl. Phys. 42 (2009) 224001.
[4] K.M. Krishnan, Biomedical nanomagnetics: a spin through possibilities in imaging, diagnostics, and therapy, IEEE Trans. Magn. 46 (2010) 2523–2558.
[5] B. Gleich, J. Weizenecker, Tomographic imaging using the nonlinear response of magnetic particles, Nature 435 (2005) 1214–12147.
[6] C. Di Rienzo, V. Piazza, E. Gratton, F. Beltram, F. Cardarelli, Probing short -range protein Brownian motion in the cytoplasm of living cells, Nat. Commun. 5 (2014) 5891.
[7] F. Höfling, T. Franosch, Anomalous transport in the crowded world of biological cells, Reports on Progress in Physics 76 (4) (2013) 046602.
[8] Albert Einstein, On the motion of small particles suspended in liquids at rest required by the molecular-kinetic theory of heat, Annalen der physik 17 (1905) 549–560.
[9] Tongcang Li, et al., Measurement of the instantaneous velocity of a Brownian particle, Science 328 (5986) (2010) 1673–1675.
[10] Simon Kheifets, et al., Observation of Brownian motion in liquids at short times: instantaneous velocity and memory loss, Science 343 (6178) (2014) 1493–1496.
[11] T. Bonchev, et al., A study of Brownian motion by means of the Mössbauer effect, Sov. Phys. JETP 23 (1966) 42–46.
[12] H. Keller, W. Kündig, Mössbauer studies of Brownian motion, Solid State Commun. 16 (2) (1975) 253–256.
[13] Katarzyna Dziedzic-Kocurek, Piotr Fornal, Jan Stanek, Mobility of interacting inorganic nanoparticles, Nukleonika 60 (1) (2015) 19–22.
[14] J. Landers, et al., Simultaneous study of brownian and neel relaxation phenomena in ferrofluids by mossbauer spectroscopy, Nano Lett. 16 (2) (2016) 1150–1155.
[15] M.E. Mobius, et al., Aging and solidification of supercooled glycerol, J. Phys. Chem. B 114 (22) (2010) 7439–7444.
[16] M.A. Chuev, et al., Separation of contributions of the magnetic relaxation and diffusion of nanoparticles in ferrofluids by analyzing the hyperfine structure of Mössbauer spectra, JETP Lett. 108 (1) (2018) 59–62.
[17] K.S. Singwi, A. Sjölander, Resonance absorption of nuclear gamma rays and the dynamics of atomic motions, Phys. Rev. 120 (4) (1960) 1093.
[18] Aleksey Nikitin, et al., Synthesis, characterization and MRI application of magnetite water-soluble cubic nanoparticles, J. Magnet. Magnet. Mater. 441 (2017) 6–13.
[19] Rene Massart, Preparation of aqueous magnetic liquids in alkaline and acidic media, IEEE Trans. Magnet. 17 (2) (1981) 1247–1248.
[20] D.H. Jones, K.K.P. Srivastava, Many-state relaxation model for the Mössbauer spectra of superparamagnets, Phys. Rev. B 34 (1986) 7542–7548.
[21] M.A. Chuev, Multilevel relaxation model for describing the Mössbauer spectra of nanoparticles in a magnetic field, JETP 114 (2012) 609–630.
[22] I. Mischenko, M. Chuev, et al., Biodegradation of magnetic nanoparticles evaluated from Mössbauer and magnetization measurements, Hyperfine Interact. 219 (2013) 57–61.
[23] M.A. Chuev, V.M. Cherepanov, M.A. Polikarpov, On the shape of the gamma resonance spectra of slowly relaxing nanoparticles in a magnetic field, JETP Lett. 92 (1) (2010) 21–27.
[24] Santoyo Salazar, Jaime, et al., Magnetic iron oxide nanoparticles in 10− 40 nm range: composition in terms of magnetite/maghemite ratio and effect on the magnetic properties, Chem. Mater. 23 (6) (2011) 1379–1386.
[25] Raul Gabbasov, et al., Mössbauer, magnetization and X-ray diffraction characterization methods for iron oxide nanoparticles, J. Magnet. Magnet. Mater. 380 (2015) 111–116.
[26] Gerardino D'Errico, et al., Diffusion coefficients for the binary system glycerol + water at 25 C. A velocity correlation study, J. Chem. Eng. Data 49 (6) (2004) 1665–1670.